Supplementary Materials for

Dopamine oxidation mediates mitochondrial and lysosomal dysfunction in Parkinson's disease

Lena F. Burbulla, Pingping Song, Joseph R. Mazzulli, Enrico Zampese, Yvette C. Wong,
Sohee Jeon, David P. Santos, Judith Blanz, Carolin D. Obermaier, Chelsee Strojny,
Jeffrey N. Savas, Evangelos Kiskinis, Xiaoxi Zhuang, Rejko Krüger,
D. James Surmeier, Dimitri Krainc*

*Corresponding author. Email: dkrainc@nm.org

This PDF file includes:

Materials and Methods
Supplementary Text
Figs. S1 to S10
References

Materials and Methods

Human iPSC culture and neural differentiation
All human iPSC lines were generated from skin fibroblasts through retroviral expression of OCT4, SOX2, cMYC, KLF4 as previously described (*25*). DJ-1 mutant lines were generated from two familial PD DJ-1 linked patients and one related heterozygous mutation carrier that were clinically characterized previously (*26*). iPSC lines from one idiopathic PD patients (iPD1), one familial PD Parkin V324A linked patient, one familial PD LRRK2 G2019S linked patient, one familial PD PINK1 Q456X linked patient, one familial PD patient harboring *SNCA* triplication and two separate healthy control subjects were previously described and characterized (*11, 15-17, 27*). Two iPSC lines were obtained from the NINDS Repository at the Coriell Institute for Medical Research (idiopathic PD patient iPD2, cat. no. ND39896; PD patient harboring *SNCA* triplication, cat. no. ND34391). No known causative *PARK* mutations were detected. Homozygous and heterozygous DJ-1 mutant iPSC lines were characterized for *in vitro* differentiation (see below) and expression of pluripotent markers by immunocytochemistry (NANOG, OCT4, SSEA4, TRA1-81) and by quantitative RT-PCR (SOX2, cMYC, OCT4, NANOG, TDG1, UFP1, DNMT3B). Total RNA was prepared using the RNeasy kit (Qiagen) and then reverse transcribed into cDNA with the SuperScript III First-Strand Synthesis System (Invitrogen). Quantitative RT-PCR was performed with SYBR GreenER (Invitrogen) on the 7500 Fast Real-Time PCR system (Applied Biosystems). All lines were routinely tested for mycoplasma contamination.

Differentiation of human iPSCs into midbrain dopaminergic neurons was done according to published protocols (*28*). To help control neuralization variability, cells were passaged en bloc (size of 1–2 mm) between d11 and d14, followed by plating onto poly-d-lysine (PDL) / laminin coated 10cm dishes. At d25 to d30, neural blocks were passed by accutase treatment onto PDL / laminin coated culture dishes. Neuralization growth factors were withdrawn at d40 and neurons were maintained in Neurobasal media (Life Technologies) containing Neurocult SM1 (Stemcell technologies). Immunocytochemistry demonstrated the neuralization efficiency in neurons derived from iPSC lines using neural (β-III-tubulin) and midbrain (TH, FOXA2, LMX1a) specific markers.

In vitro differentiation
Human iPSC colonies were detached using 2 mg/mL collagenase IV. Embryoid bodies (EBs) formation was initiated by culturing the colonies in suspension on non-treated tissue culture dishes in iPSC medium in the absence of bFGF for 7 days. On day 7, EBs were picked and plated onto PDL/laminin-coated coverslips and cultured for 7 days in DMEM KO media (ThermoFisher Scientific) supplemented with 10% fetal calf serum and 1% penicillin/glutamine. Cultures were then fixed and stained with primary antibodies as indicated.

Human DJ-1 KO isogenic lines
CRISPR guides were designed using the Zhang Lab CRISPR Design Tool (crispr.mit.edu). Guides were selected that had high predicted activity and had off-targets with at least 3-bp mismatches in coding regions and at least 2-bp mismatches in non-

coding regions. Guides were cloned into pSpCas9(BB)-2A-GFP (pX458, Addgene #48138) using standard protocols. Control iPSC were grown to confluence in 10 cm plates. Once confluent, cells were dissociated using TrypLE Express (Life Technologies). 5 million cells were transfected with 3 µg of 3 unique CRISPR plasmids all targeting within the first coding exon of PARK7 (1 µg of each CRISPR plasmid was used). The transfection was done using the NEON Transfection System (Invitrogen) using a single 1400 V, 20 ms pulse. Cells were plated in mTeSR + 10 µM ROCK inhibitor (DNSK International). 48 hours later, cells were sorted on a BD FacsAria SORP and the top 30% GFP+ cells were collected and plated for expansion. Once confluent, the cells were replated at clonal density in a 10 cm plate (10,000-20,000 cells per well) and grown until individual colonies were visible to the naked eye. Individual colonies were picked into single wells of a 48-well plate. These cells were grown to confluence and the plates were then duplicated. One of these plates was used for extraction of genomic DNA and a PCR-based approach was employed to identify cells containing indels. PCR products from clones of interest were then TOPO TA subcloned and sequenced to a depth of 10X to identify the exact nature of the mutations. The second plate was used for expansion of clones of interest upon PCR genotyping and sequencing.

Off target gene editing was assessed by using a T7 endonuclease I (T7E1) assay in the regions of highest homology to the targeted DNA sequence in DJ-1. Genomic DNA from both control and targeted cell lines was amplified by PCR using specific sets of primers for the DNA elements with the highest homology to DJ-1. PCR products were then denatured and re-annealed leading to the formation of homo and heteroduplexes, detectable by digestion with T7E1 that recognizes and cleaves mismatched DNA. The resulting cleaved and full-length PCR products were visualized by gel electrophoresis.

Mouse iPSC culture and neural differentiation

Mouse iPSC lines were generated from WT and DJ-1 KO mouse embryonic fibroblasts through Sendai virus reprogramming vectors OCT4, SOX2, cMYC and KLF4. Both mouse iPSC lines expressed pluripotency markers. Differentiation of mouse iPSCs into midbrain dopaminergic neurons was done according to published protocols (29). Briefly, undifferentiated iPSCs were grown on gelatin-coated tissue culture plates in stem cell media containing leukemia inhibitory factor (LIF). To induce embryoid body (EB) formation, the cells were washed and dissociated into a single-cell suspension by incubating in trypsin/EDTA (0.05%/0.53mM) and plated onto ultra-low attachment flasks. The EBs were formed in stem cell medium for 4 days and then plated onto fibronectin-coated tissue culture surfaces in stem cell medium. After 24h, the medium was replaced by serum-free medium containing insulin, transferrin and selenium. After 6-8 days cells were dissociated by trypsin/EDTA (0.05%/0.53mM) and plated onto PDL/laminin-coated tissue culture plates or glass coverslips in serum-free medium containing insulin, transferrin, selenium, putrescine and progesterone supplemented with 10 ng/ml of bFGF in the presence of murine N-terminal fragment of SHH and murine FGF8. Cells were expanded for 4-6 days. Final differentiation was induced by removal of bFGF, SHH and FGF8. The final differentiation medium contained insulin, transferrin, selenium, putrescine and progesterone supplemented with cAMP and AA. The cells were cultured under differentiation conditions until day 25 of differentiation, when the neutralization factors were withdrawn.

WT and DJ-1 KO transgenic mice
Wildtype C57BL/6 mice (Charles River) and *DJ-1⁻/⁻* (T. Dawson) mice back-crossed onto the C57BL/6 line were bred following Institutional Animal Care and Use Committee at Northwestern University guides and handled in accordance with the US National Institutes of Health Guide to the Care and Use of Laboratory Animals and Society for Neuroscience guidelines.

DASYN53 x DJ-1 KO transgenic mice
DJ-1 KO mice (*30*) were crossed with DASYN53 double-transgenic mice (*23*) to generate DASYN53 x DJ-1 KO triple-transgenic mice. Briefly, we used a tetracycline inducible system-based "PF" strategy with amplified expression limited to dopamine (DA) neurons. The Tet operator (tetO)- tetracycline responsive transactivator (tTAt) "PF" cassette was inserted between the DA transporter (DAT) gene promoter and the coding sequence via gene targeting. With this "PF" design, the tetO promoter directs the expression of tTA, which in turn activates the tetO promoter. However, the "PF" cassette by itself has no transcription activity unless it is initiated by tTA expression from another promoter. Therefore, an additional tTA was inserted right downstream of the DATpromoter and upstream of the "PF" cassette. The gene targeting construct also contains a transcriptional "stop" and a floxed PGK-neo cassette for selection during embryonic stem (ES) cell culture. In this DAT-PF-tTA line, the DAT promoter initiates and directs tTA expression only in DA neurons. tTA expression level is then further amplified by the "PF" cassette. Primogenix PRX-129/S6 ES cells were used for targeting. Male chimeras were crossed with a germ line deleter, Meox2-cre (The Jackson Laboratory), to remove the PGK-neo cassette. The resulting DAT-PF-tTA line was crossed with the Tg(tetO-SNCA_A53T)E2Cai/J line obtained from The Jackson Laboratory (*31*) to generate DASYN53 double-transgenic mice.
All animal procedures were approved by the Institutional Animal Care and Use Committee at the University of Chicago.

L-DOPA diet of WT and DJ-1 KO transgenic mice
WT as well as DJ-1 KO mice were provided with L-DOPA-supplemented or vehicle-treated chow either once a week for 24h for a duration of 6 months (until 14 months of age) or daily for 30 days (until 3-5 months of age).

Mitochondrial roGFP imaging
Neurons were transduced with AAV containing the mitochondrial roGFP construct with a CMV promoter and a mitochondrial-matrix-targeting sequence (mito-roGFP, (*5*)) at MOI 10 and experiments were done 5 days post infection. Neurons expressing mito-roGFP were visualized using epifluorescence microscopy (excitation wavelength 410 and 470 nm, emission was monitored at 535 nm) as recently described (*5, 32*). Relative oxidation was determined from fluorescence measurements after reducing mitochondria with dithiothreitol (DTT) and then oxidizing with Aldrithiol (ALD). Because the calibrated signal becomes independent of the absolute expression level of mito-roGFP, this strategy allows cell-to-cell comparisons.
The relative oxidation was calculated as $1 - [(F - F_{Ald})/(F_{DTT} - F_{Ald})]$.

Sequential biochemical extractions in iPSC-derived neurons

Neurons were scrapped in cold PBS and centrifuged at 400x g for 5 min. PBS was removed and the cell pellet was homogenized in 1% Triton X-100 lysis buffer (containing 10% glycerol, 150mM NaCl, 25mM Hepes pH7.4, 1mM EDTA, 1.5mM MgCl$_2$, proteinase inhibitor cocktail) as described previously (*14*) (T-soluble fraction). Insoluble pellets from a 100,000x g spin were further extracted in 2% SDS/50mM Tris pH 7.4 by boiling and sonication (T-insoluble fraction). Samples were loaded onto SDS-PAGE gels followed by western blot analysis or further extracted for nIRF assay (see below). Depending on the experiment, cells were treated with the following reagents: mito-TEMPO (10μM, 30 days), NAC (500μM, 30 days), AMPT (500μM, 30 days), Isradipine (500nM, 30 days), FK506 (100nM, 30 days), L-DOPA (50μM, 20 days in human neurons; 50μM, 15 days in mouse neurons).

Near infrared fluorescence (nIRF) detection of oxidized dopamine

Neurons were scrapped in cold PBS and centrifuged at 400x g for 5min. The cell pellet was homogenized in 1% Triton X-100 lysis buffer (containing 10% glycerol, 150mM NaCl, 25mM Hepes pH7.4, 1mM EDTA, 1.5mM MgCl$_2$, proteinase inhibitor cocktail). To analyze brain tissue, freshly dissected tissue from different regions of DJ-1 KO and widtype mice were homogenized in 1% Triton X-100 lysis buffer according to tissue weight. Insoluble pellets from a 100,000x g spin (30min, 4°C) were extracted in 2% SDS/50mM Tris pH 7.4 by boiling and sonication. SDS buffer volume per sample was normalized according to protein concentration of the T-soluble fraction. Leftover insoluble pellets from a 150,000x g spin (30min, 4°C) were further extracted in 1N NaOH (half the volume of the SDS buffer volume) and incubated at 55°C overnight. The volume of NaOH for extraction was calculated depending on the protein concentration of the soluble fraction. To ensure complete solubilization, the solution was again sonicated or vortexed depending on the amount and maturity of the dopamine quinone (DAQ)-protein adducts and neuromelanin. The solution was then lyophilized in a Speed Vac Concentrator until the pellet was completely dry. The pellet was washed once with Nanopure H$_2$O for removal of hydroxides and to lower pH levels, and then lyophilized again before the dried pellet was taken up in Nanopure H$_2$O and finally analyzed. The standard was made from a 10mM oxidized dopamine (DA) stock. For preparation of oxidized DA, 10mM DA (in D-PBS) was mixed with 20mM NaIO$_4$ (in D-PBS), vortexed briefly and incubated for 5min at RT. The solution was then handled in the same way as the cell samples including centrifugation, sonication and lyophilization steps. The final pellet was taken up in Nanopure H$_2$O and standard dilution prepared.

10μl of each sample or standard dilution was dropped onto a Biodyne Nylon Transfer Membrane (Pall, #Pall-60209) and membranes were scanned using an Odyssey infrared imaging system (Li-Cor) with the 700 channel. Samples were quantified by obtaining integrated spot intensities using Odyssey infrared imaging software, version 3.1 (Li-Cor). For in-gel nIRF detection, loading buffer was added and protein samples were heated at 95°C for 5min before loading onto NuPAGE Tris-glycine gels (Life Technologies). After completion of the run, gels were scanned using an Odyssey infrared imaging system (Li-Cor) with the 700 channel for detection of protein modified by oxidized catechols. Gels were then stained with Coomassie Brilliant Blue (CBB) to visualize total protein.

Determination of oxygen consumption rates (OCR)
Mitochondrial OCR was determined as described previously using the XF24 Extracellular Flux Analyzer (Seahorse Bioscience) (16). On the day of experiment, culture media was replaced with fresh media before plates were preincubated in a CO_2-free incubator at 37°C for 1 h for equilibration before processing in the XF24 Extracellular Flux Analyzer (Seahorse Bioscience). For baseline measurements, a 20 min equilibration step was followed by three cycles of 2 min mix, 3 min wait, and 2 min measurement time. For analysis of drug response, three cycles of 2 min mix, 3 min wait, and 2 min measurement were used per condition. After three baseline measurements were taken, oligomycin (1µM), CCCP (1µM), and antimycin A (1µM) were added sequentially, with three measurements per condition. For normalization of cell number, cells were harvested after the experiment in RIPA buffer and protein concentration was measured.

General Oxidative Stress Assay using CM-H2DCFDA probe
CM-H_2DCFDA (2',7'-dichlorodihydrofluorescein diacetate) (Thermo Fisher Scientific) was used in cultured cells as a general organelle-nonspecific cell-permeant indicator of reactive oxygen species (ROS) including hydrogen peroxide, hydroxyl radical, carbonate radical and nitrogen dioxide, according to manufacturer's instructions. CM-H_2DCFDA was used at 5µM with an incubation time of 10 min.

Electron microscopy
Neurons were fixed with 2.5% glutaraldehyde in 0.1 M sodium cacodylate buffer, pH 7.3 for 1h, rinsed several times with PBS followed by post fixation with 1% osmium tetroxide in PBS for 1h. Specimens were rinsed again with PBS for 15min and then dehydrated through a series of graded ethyl alcohols from 50 to 100%. Specimens were finally embedded and resin blocks sectioned. Samples were imaged on a FEI Tecnai Spirit G2 transmission electron microscope.

Lysosomal proteolysis in live neurons and lysosomal enzyme activity assays
Long-lived protein degradation assay was performed by radioactive pulse-chase using tritium-labeled leucine (Perkin-Elmer, #NET460A001MC) as previously described (33). Briefly, proteins were labeled with radioactive leucine for 36 hrs (pulse period), followed by a chasing period of 28 hrs. Short-lived proteins were excluded from the analysis by replacing the media after one hour of chasing period with fresh chasing media. For lysosomal inhibition, 100 mM of leupeptin was added to the initial medium (pulse period) and 100 mM of leupeptin and 5 mM of NH_4Cl were added to the chasing medium. Aliquots of culture media were sampled after 8, 20 and 28 hours during chasing period and precipitated with 20% v/v trichloroacetic acid with 0.5mg/ml BSA for a minimum of 8 hrs at 4°C followed by centrifugation at 20,000 x g, 20 min, 4°C. Pellets were resuspended in 0.1 N NaOH / 0.1% NaDexoycholate. After the last time point, cells were scrapped and harvested in 0.1 N NaOH / 0.1% NaDexoycholate. Radioactive counts of cell lysates and secreted proteins were measured using a liquid scintillation analyzer (TriCarb 2800TR, Perkin Elmer). Percentage of secreted proteins was determined by dividing the radioactive signal obtained from the media by the total radioactive counts obtained from the cell lysate. Lysosomal proteolysis was calculated as the difference

between control and inhibited conditions. Treatment with NAC (500μM) was done for 140 days. Media was replaced every three days.

Enzyme activity assays were performed using the artificial enzyme substrates 4MU-glucopyranoside (for GCase) and 4MU-sulfate potassium salt (for a-i-2-sulf) as previously described (*14*). 5ug cell lysate was added to 10μl of 10% BSA (in activity assay buffer: 0.25% (v/v) Triton X-100 (Sigma-Aldrich # T-8787)) and to 20μl of 5mM artificial enzyme substrate (in activity assay buffer). The mixture was added up to 100ul total with activity assay buffer, 0.25% (w/v) Taurocholic acid (Sigma-Aldrich, # T9034), 1 mM EDTA, in citrate/phosphate buffer (pH 5.4). Samples were mixed and incubated at 37°C for 30 min. The reaction was stopped by adding 100μl of stop solution (1M glycine, pH 12.5) to each sample. Samples were loaded into a 96-well fluoro plate (F16 Black Maxisorb Plate, Nunc # 475515) and fluorescence was recorded using a spectramax i3 plate reader (Molecular Devices) (Ex=365nm, Em=445nm; top read).

Generation of lysosomal-enriched fractions

Subcellular fractionation to obtain lysosomal fractions was performed as previously described (*14*). Briefly, cells were harvested in sucrose buffer (0.25 M sucrose, 10 mM HEPES pH 7.4, 10M EDTA), homogenized, and centrifuged at 6,800g at 4°C for 5 min. This step was repeated, the supernatant from both extractions combined and centrifuged again at 20,000g, at 4°C for 10 min. The supernatant was removed and the remaining pellet enriched in lysosomes was extracted in 1% Triton X-100 lysis buffer and then further analyzed.

Calcineurin activity assay

Calcineurin Cellular Activity Assay Kit (#BML-AK816, Enzo) was used in cultured cells to measure cellular calcineurin phosphatase activity according to manufacturer's instructions. 2μg of total protein was used per sample.

Cell-free *in vitro* assays with recombinant protein

For in-gel nIRF detection as well as for mass spectrometry experiments, proteins were purified using an Amicon Ultra-0.5 Centrifugal Filter Unit with Ultracel-10 membrane (EMD Millipore # UFC501096) and incubated with DA hydrochloride (Sigma Aldrich # H8502) in a 1:5 ratio (protein/DA ratio) according to its molecular weight or PBS at 37°C for 48hrs. For NAC treatment, 500 μM NAC was added to the sample during the incubation at 37°C for 48h. Removal of free DA after incubation step was accomplished in Amicon Ultra-0.5 Centrifugal Filter Units with Ultracel-3 membrane (EMD Millipore # UFC500396).

Mass spectrometry

Precipitated proteins were denatured with 8M urea and ProteasMAX (Promega) following the manufacturer's instructions. The proteins were then reduced with 5 mM Tris(2 carboxyethyl)phosphine at RT, alkylated in the dark by 10 mM iodoacetamide for 20min, and the reaction was stopped by using 50mM ammonium bicarbonate and 500mM Tris(2 carboxyethyl)phosphine before being digested with Trypsin (Promega) overnight at 37°C. The peptides were desalted with C18 RP spin columns (Pierce) and dried, and reconstituted in 5% (vol/vol) acetonitrile/0.125% formic acid. 3ug of peptide

was then analyzed with an Orbitrap Fusion Tribrid mass spectrometer and the spectra was subjected to a standard database search.

UPLC and mass spectrometry operation
The peptides were loaded onto a C18 RP trap column (Acclaim PepMap 100) washed and then transferred to a 50cm C18 RP analytical column (Acclaim PepMap RSLC) directly in line with an Orbitrap Fusion Tribrid mass spectrometer. The buffer solutions used were 5% (vol/vol) acetonitrile/0.125% formic acid (buffer A), 99.875% (vol/vol) acetonitrile/0.125% formic acid (buffer B). The LC method consisted of a gradient from 0-7% B from time = 0–3 minutes, 7-10% B from 3-6 min, 10-25% from 6-86 min, 25-33% from 86-106 min, 33-50% from 106-109 min, 50-95% from 109-112 min, and 95% from 112-120 min. Some samples were analyzed for 240 min, with similar chromatography parameters.   As peptides eluted from the microcapillary column, they were electrosprayed into the MS with the Nanospray Flex ion source with a distal 2.5-kV spray voltage. A cycle of one Oribtrap full-scan mass spectrum (300–1,500 m/z) at a resolution of 60,000 followed by 20 data-dependent MS/MS spectra in the ion trap at 30% normalized collision energy was repeated continuously throughout each step of the separation. For the orbitrap full scan, max ion accumulation time was set for 50 ms, AGC target = 200K, with ETD internal calibration, and 1 micro scan. For the ion trap MS, max ion accumulation time was set for 75ms, AGC target = 10K, and 1 micro scan. Charge state rejection was set to omit singly charged ion species and ions for which a charge state could not be determined for MS/MS. We considered only charges 2-6, and minimal signal for fragmentation was set to 1,000. Dynamic exclusion was enabled with a repeat count of 1, an exclusion duration of 45.00 s, and exclusion mass with high/low of 10.00 ppm. The mass spectrometer scan functions and nLC1000 solvent gradients were controlled by the Xcaliber data system.

Analysis of Tandem mass spectrometry
Protein identification and quantification and analysis were done with Integrated Proteomics Pipeline - IP2 (Integrated Proteomics Applications, Inc., www.integratedproteomics.com/) using ProLuCID and DTASelect2. Spectrum raw files were extracted into ms1 and ms2 files from raw files using RawExtract 1.8 (http://fields.scripps.edu/downloads.php) , and the tandem mass spectra were searched against the UniProt Human Proteome Construct Database (downloaded on March 25, 2014). To estimate peptide probabilities and FDRs accurately, we used a target/decoy database containing the reversed sequences of all the proteins appended to the target database (*34*). Tandem mass spectra were matched to sequences using the ProLuCID algorithm with 50 ppm peptide mass tolerance for precursor ions and 400 ppm for fragment ions. ProLuCID searches were done on an Intel Xeon cluster running under the Linux operating system. The search space included all fully and half-tryptic peptide candidates that fell within the mass tolerance window with no miscleavage constraint. The addition of iodoacetamide adduct (57.02146 Da) was considered a static modification on cysteine residues and DAQ (+151.06332 Da) on cysteine residues was considered as a differential modification. We required at least 1 trypic terminus, and unlimited miss cleavages. The validity of peptide/spectrum matches (PSMs) was assessed in DTASelect using two SEQUEST (*35*) -defined parameters, the cross-correlation score

(XCorr), and normalized difference in cross-correlation scores (DeltaCN). A peptide confidence of 0.95 was set as the minimum threshold. The FDR was calculated as the percentage of reverse decoy PSMs among all the PSMs that passed the confidence threshold. Each protein identified was required to have a minimum of one peptide; however, this peptide had to be an excellent match with an FDR less than 0.001 and at least one excellent peptide match. After this last filtering step, we estimate that both the protein FDRs were below 1% for each sample analysis. The search results were grouped by DA incubation conditions compared against PBS incubation conditions, which were searched with identical search and filtering parameters. Detailed search results are as follows: Glucocerebrosidase=K.SYFSEEGIGYNIIRVPMASC(151.06332)DFSIR.T, Xcorr = 6.0397, DeltaCN = 0.4037, delta mass (ppm) = -9.9.

Electrophysiological recordings
For patch-clamp recordings coverslips were transferred to a chamber perfused by gravity at 2 mil/min with ACSF containing (in mM): 125 NaCl, 25 NaHCO3, 2.5 KCl, 1.25 NaH2PO4, 2 CaCl2, 1 MgCl2, and 25 glucose, bubbled with a mixture of 95% O2 and 5% CO2 at 33-34°C. Patch pipettes (3-3.5 MΩ) pulled from borosilicate glass were filled with internal solution containing (in mM): 135 K-MeSO4, 5 KCl, 5 HEPES, 0.05 EGTA, 10 Phosphocreatine-di(tris), pH 7.3 (290–300 mOsm). The patch pipette was tip-filled with internal solution and back-filled with internal solution containing gramicidin (Sigma-Aldrich, working concentration 20μg/ml). Cells were visualized by infrared differential interference contrast video microscopy and electrophysiological recordings were filtered at 1–4 kHz and digitized at 5–20 kHz with a Digidata 1400 (Molecular Devices) and collected via the PrairieView 5.2 electrophysiology application.

Western blot analysis
Neurons were scrapped in cold PBS and centrifuged at 400x g for 5 min. PBS was removed and the cell pellet was homogenized in 1% Triton X-100 lysis buffer (containing 10% glycerol, 150mM NaCl, 25mM Hepes pH7.4, 1mM EDTA, 1.5mM MgCl$_2$, proteinase inhibitor cocktail) as previously described (*14*). For western blot analysis of brain tissue from DJ-1 KO and WT mice, freshly dissected tissue was homogenized in 1% Triton X-100 lysis buffer according to tissue weight. Insoluble pellets from a 100,000 x g spin were further extracted in 2% SDS/50mM Tris pH 7.4 by boiling and sonication. Lysates were analyzed by western blot, blocked in Odyssey Blocking Buffer (LI-COR Biosciences), and incubated with the following primary antibodies: α-synuclein (LB509, Life technologies, 1:500; syn211, Sigma-Aldrich #S5566, 1:1000; C-20, Santa Cruz #SC-7011-R, 1:1000; syn303, BioLegend #MMS-5085, 1:500; syn202, #MMS-529R, 1:1000), DJ-1 (abcam, #ab18257, 1:1000), oxidized DJ-1 (abcam, #ab169520, 1:500), synapsin (Santa Cruz, #sc-398849, 1:1000), calcineurin (abcam, #ab3673, 1:1000), tyrosine hydroxylase (TH) (EMD Millipore, #657012, 1:1000), β-III-tubulin (Covance, 1:5000), GAPDH (Millipore #MAB374, 1:5000), β-actin (abcam, #ab11003, 1:5000), vimentin (1:5000), α-tubulin (Sigma, #t5168, 1:5000), neural specific enolase (Pierce #PA5-12374, 1:1000). Syn303 antibody was used to detect oxidized forms of α-synuclein as previously described (*36*).

Immunofluorescence analysis
Neurons were fixed in 4% paraformaldehyde and permeabilized with 0.3% Triton X-100 in PBS. Cells were blocked in 1-2% BSA, 5% normal goat serum in PBS-Triton for 30 min and the following primary antibodies were used: anti β-III-tubulin (Covance, #MMS-435P, 1:1000 or Covance, #MRB-435P, 1:1000), tyrosine hydroxylase (EMD Millipore, #657012, 1:1000), HNF-3 beta (FOXA2) (Santa Cruz, #sc-101060, 1:100), LMX1A (EMD Millipore, #AB10533, 1:1000), NANOG (Abcam, #ab80892, 1:1000), OCT4 (Abcam, #ab19857, 1:300), SSEA4 (Merck KGaA, #MAB4304, 1:100), TRA-1-81 (Merck KGaA, #MAB4381, 1:50), AFP (Sigma Aldrich, #A8452, 1:100), SMA (Dako, #M0851, 1:100). Primary antibodies were incubated overnight, washed in PBS and incubated with Alexa-conjugated anti-rabbit or anti-mouse antibodies at 1:500. Images were analyzed and captured at equal exposure times. For quantification, the number of cells was normalized to total cells in the field of view (calculated by nuclear DAPI stain). At least 3 fields of view were analyzed per coverslip.

Determination of dopamine and metabolites by HPLC with electrochemical detection
Measurement of levels of dopamine, L-DOPA and DOPAC was performed using reversed-phase HPLC with electrochemical detection. Human and mouse neurons were harvested in 50ul of 0.1M perchloric acid containing 100nM 3,4 dihydroxybenzylamine (DHBA). Cell lysates were homogenized and centrifuged at 16,000g for 10 min at 4°C. Supernatants were filtered through 0.22 μm membranes, and 40ul per sample was injected on the HPLC for analysis of dopamine levels and metabolites using an Agilent (Palo Alto, CA) 1200 series HPLC controlled by ChemStation software (Agilent). Catechols were resolved on a reverse-phase C18 ZORBAX Eclipse XDB column (150 mm x 4.6 mm, 5 μm; Agilent, Santa Clara, CA) at a flow rate of 1 ml/min in a mobile phase consisting of 66mM citric acid, 34mM sodium phosphate, 2%methanol, and 0.04% sodium azide, pH2.0, and detected using a Coularray detector (Thermo Scientific) with the following working potentials (in mV): -200, +200, +300, and +400. Quantification of dopamine and metabolites was done by comparing the peak areas of a known amount of standards and using CoulArray Data Station software (version 3.00). Concentration of total protein was used for normalization.

Quantitative determination of homocysteine levels
Supernatants of homogenates derived from nigral tissue of WT and DJ-1 KO mice fed with L-DOPA-supplemented chow or vehicle-treated chow were analyzed for homocysteine levels using an immunoassay kit with a detection range of 0.78-50ng/ml according to manufacturer's instructions (amsbio, # AMS.E0772Ge). 50ug was used per sample.

Statistical analysis
Comparison of multiple groups was performed using one-way ANOVA followed by post-hoc Tukey test; comparisons between two groups were performed using Student's t-test. *P* values less than 0.05 were considered significant. Statistical calculations were performed with GraphPad Prism Software, Version 5.0 (http://www.graphpad.com/scientific-software/prism/). All data shown is representative

of experiments from n≥3 biologically independent samples (as detailed in figure legends). All errors bars shown in the figures are standard error of the mean (SEM).
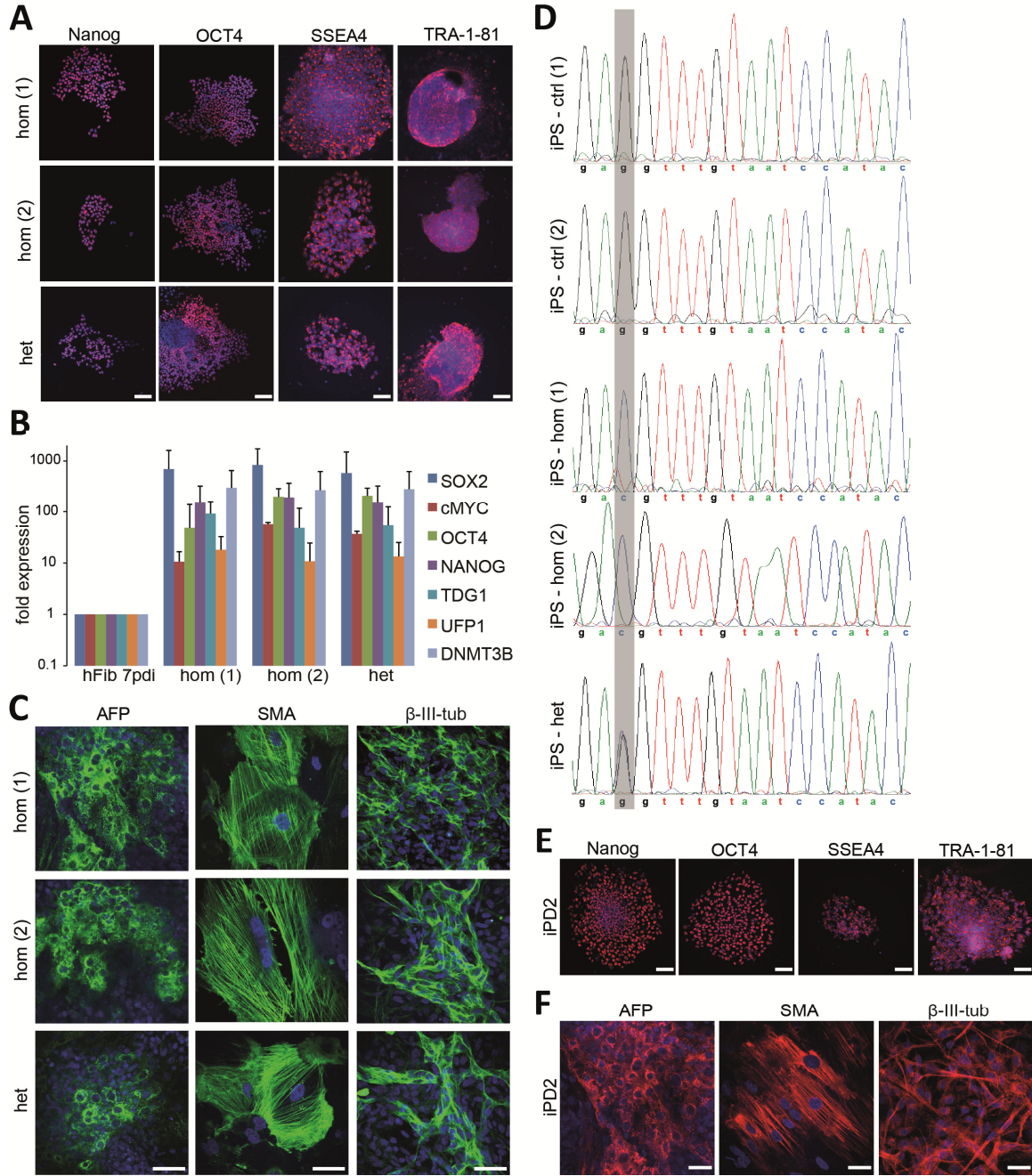
Fig. S1

Fig. S1: Characterization of homozygous and heterozygous DJ-1 mutant and sporadic PD iPSC lines. (A) Immunocytochemistry for pluripotency markers NANOG, OCT4, SSEA4 and TRA-1-81 and nuclear counterstaining with DAPI in iPSCs from heterozygous and homozygous DJ-1 mutant lines. Scale bar, 100μm. **(B)** qRT-PCR analysis for the expression of the indicated pluripotency markers (fold expression) in comparison to human skin fibroblasts at 7 days after retroviral infection. Relative expression was calculated using β-actin as housekeeping gene. **(C)** *In vitro* differentiation

via embryoid body formation and immunostaining for AFP (endoderm), SMA (mesoderm), and β-III-tubulin (ectoderm) in homozygous and heterozygous DJ-1 mutant iPSC lines. Scale bar, 50μm **(D)** Direct sequencing confirmed the *DJ-1* mutation c.192G>C in homozygous and heterozygous DJ-1 mutant iPSC lines. **(E)** Immunocytochemistry for pluripotency markers NANOG, OCT4, SSEA4 and TRA-1-81 and nuclear counterstaining with DAPI in iPSC from a sporadic PD line (iPD2). Scale bar, 100μm. **(F)** *In vitro* differentiation via embryoid body formation and immunostaining for AFP (endoderm), SMA (mesoderm), and β-III-tubulin (ectoderm) in iPSC from a sporadic PD line (iPD2). Scale bar, 100μm.
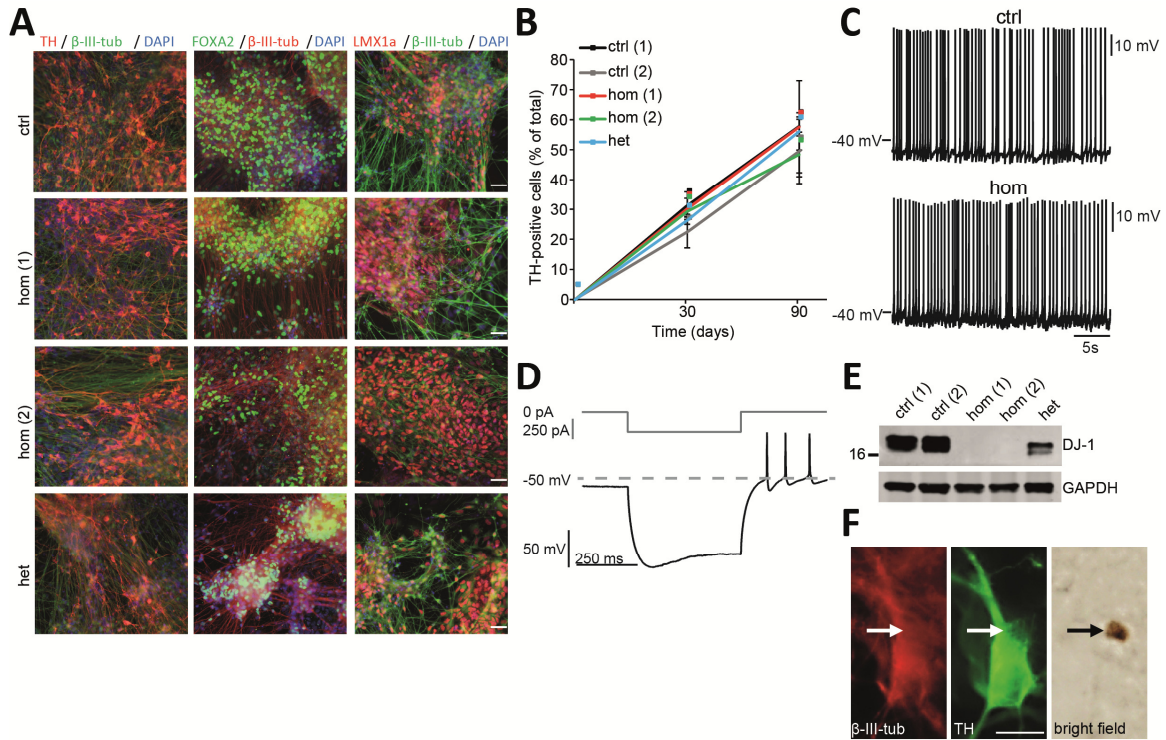
Fig. S2

Fig. S2: Characterization of homozygous and heterozygous DJ-1 mutant and control dopaminergic neurons. (**A**) Immunocytochemistry of dopamine, midbrain and neuronal markers in iPSC-derived dopaminergic neurons from DJ-1 mutant and control lines at d30. Antibodies against TH, FOXA2, LMX1a and β-III-tubulin were used. Scale bar, 20μm. (**B**) Quantification of TH-positive neurons as percent of total number of cells at d30 and d90. (**C**) Detection of low frequency pacemaker activity by current-clamp (perforated patch configuration) electrophysiological recordings in control (ctrl) and homozygous DJ-1 mutant (hom) neurons at d70. (**D**) Current clamp recordings (perforated patch configuration) in differentiated neurons showing the voltage sag and short rebound delay characteristic of SNc dopaminergic neurons upon brief injection of a strong hyperpolarizing current (-250 pA). (**E**) Immunoblot analysis confirmed DJ-1 protein levels in T-soluble neuronal lysates from homozygous and heterozygous DJ-1 mutant as well as control lines at d70. GAPDH was used as loading control. (**F**) Immunofluorescence showing a neuromelanin-like pigmented granule (bright field) in a TH (green)- and β-III-tubulin (red)-positive homozygous DJ-1 mutant neuron. Scale bar, 5μm.

Fig. S3

A

B

C
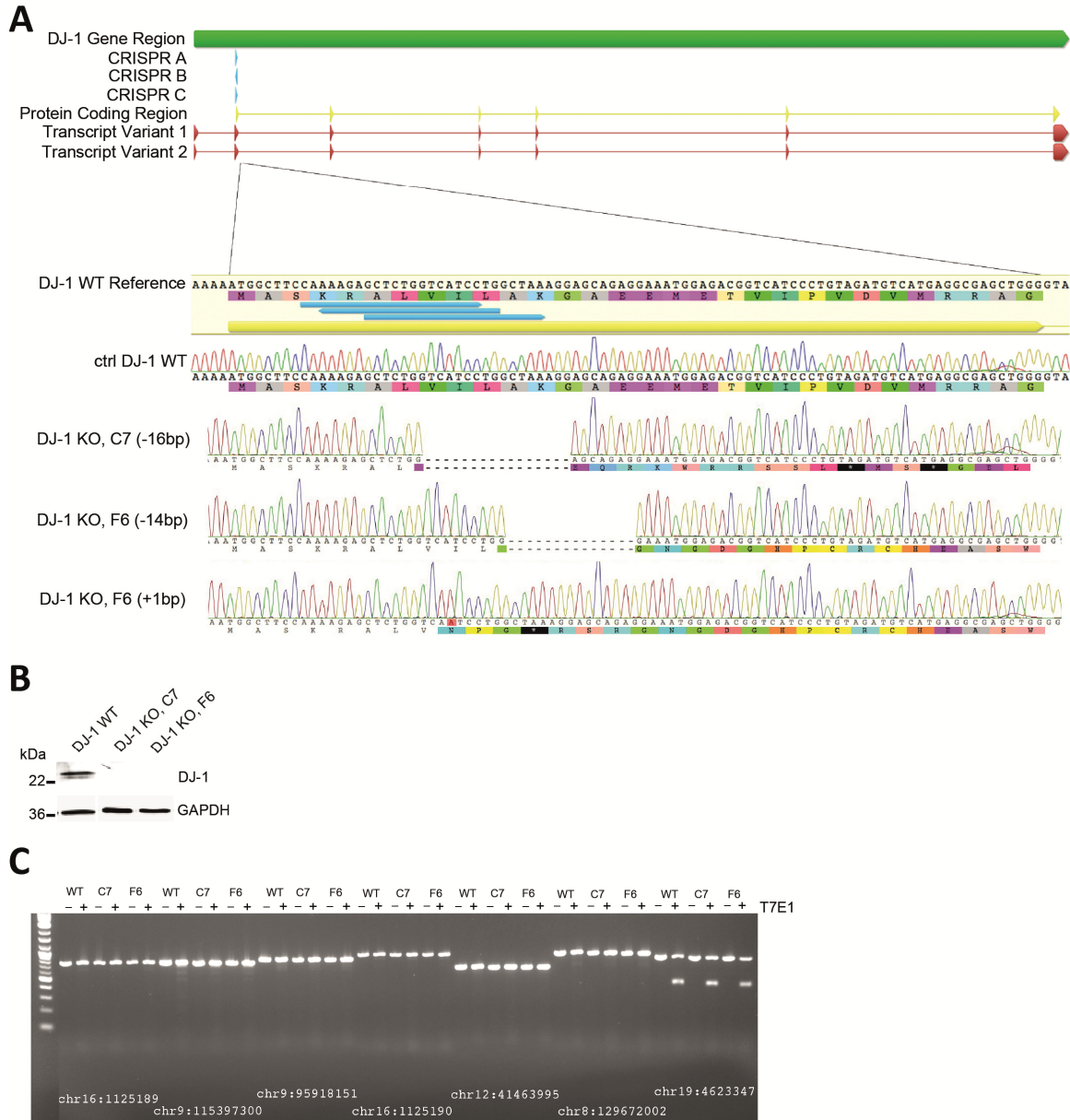
Fig.S3: CRISPR/Cas9 gene editing of human control iPSCs. (**A**) Structure of the *DJ-1* gene and schematic overview of gene targeting strategy to delete *DJ-1*. 3 unique CRISPR plasmids all targeting the first coding exon of *DJ-1* were used to generate homozygous DJ-1 KO clones. 10x sequencing analysis shows a homozygous 16bp deletion for the CRISPR-edited DJ-1 KO line 'clone C7' and a 14bp deletion as well as a 1bp insertion for CRISPR-edited DJ-1 KO line 'clone F6'. (**B**) Immunoblot analysis for the detection of DJ-1 protein in the DJ-1 WT line and the two CRISPR-edited DJ-1 KO lines 'clone C7' and 'clone F6'. (**C**) Agarose gel electrophoresis of PCR products after digestion with T7E1. No differences were detected between the parental (WT) and either one of the targeted isogenic clones (C7, F6), in any of the top seven regions of highest homology to the *DJ-1* targeted DNA sequence.

Fig. S4
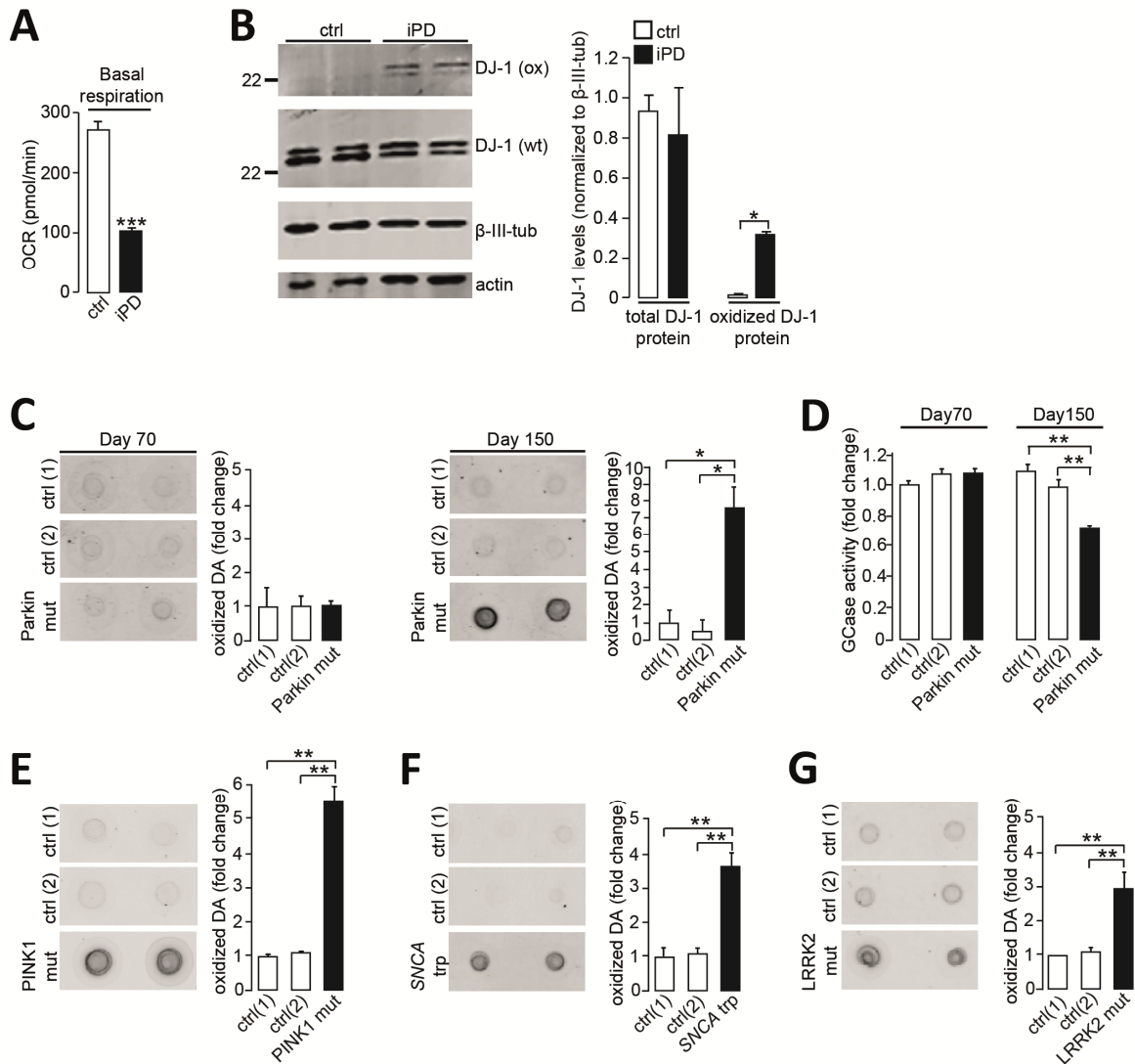
Fig. S4: Pathological phenotypes in neurons from patients with sporadic PD and familial forms of PD. (A) Quantification of OCR under basal conditions in idiopathic PD (iPD) neurons compared to control (ctrl) neurons at d50 (n=3). **(B)** Immunoblot analysis of total (wt) and oxidized (ox) DJ-1 protein extracted from control (ctrl) and idiopathic PD (iPD) human dopaminergic neurons at d70. Representative blot shows two biological replicates. β-III-tubulin and actin were used as loading controls (n=3). **(C-D)** Parkin V324A mutant neurons and control neurons were analyzed at d70 and d150 for (C) oxidized dopamine (DA) by nIRF and (D) GCase activity in lysosomal fractions. **(E-G)** Oxidized dopamine was analyzed in (E) PINK1 Q456X mutant and control neurons at d120 (n=5), (F) α-synuclein triplication and control neurons at d90 (n=3) and (G) LRRK2 G2019S mutant and control neurons at d100 (n=3). Equal protein concentrations were used for nIRF assays. Error bars, mean ± SEM. *$P<0.05$, **$P<0.01$, ***$P<0.001$, Student's t-test (A-B) or one-way ANOVA with Tukey post-hoc test (C-G).

Fig. S5
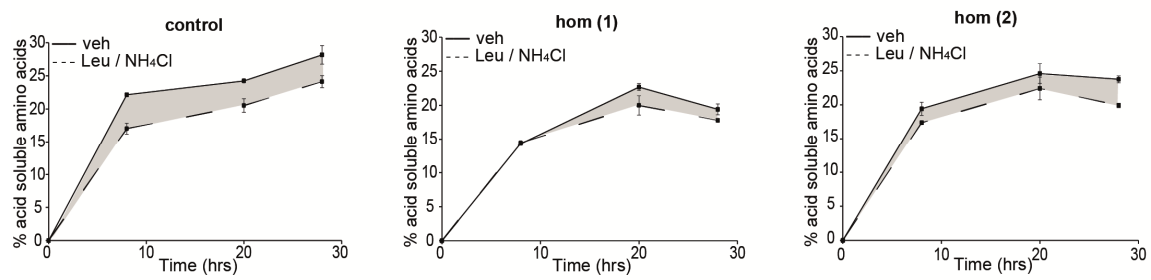
Fig. S5: Lysosomal proteolysis in homozygous DJ-1 mutant neurons. Proteolysis of long-lived proteins occurring within lysosomes was determined as the area under the curve (shaded area) of vehicle-treated (solid line) and lysosome-inhibited (dashed line) conditions for two homozygous DJ-1 mutant lines and one control line at d180.
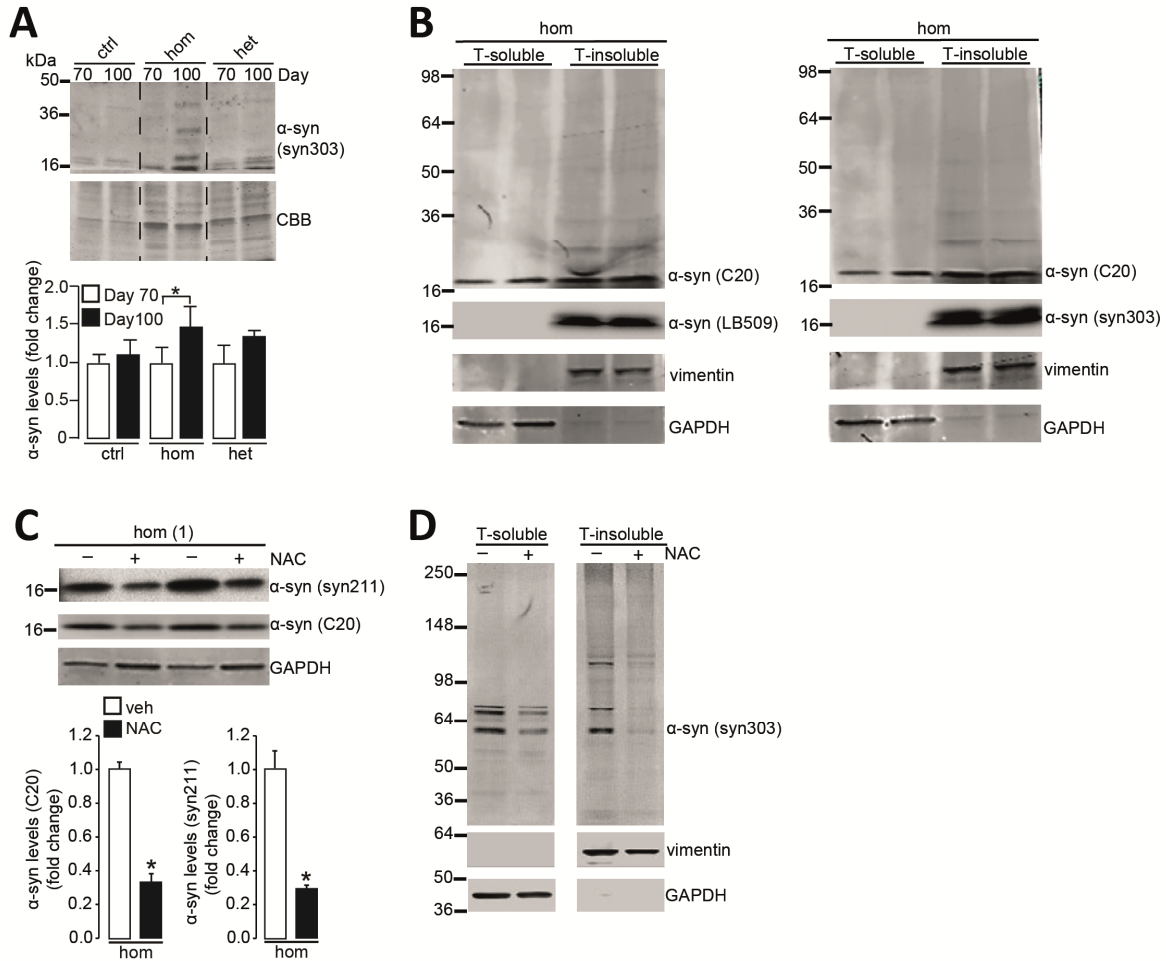
Fig. S6

Fig. S6: α-Synuclein accumulation in homozygous DJ-1 mutant neurons is rescued by antioxidant treatment. (A) Immunoblot analysis of T-insoluble oxidized α-synuclein (syn303 antibody) at d70 and d100. Quantification is normalized for each line to d70 time point. CBB was used as loading control (n=4). **(B)** T-soluble and T-insoluble α-synuclein extracted from neuronal lysates of a homozygous DJ-1 mutant line using anti- α-synuclein antibodies C20 and LB509 (left) or C20 and syn303 (right) showing an increase in T-insoluble forms of α-synuclein compared to soluble α-synuclein in older cultures (d150). Vimentin and GAPDH were used as loading controls. **(C)** T-soluble α-synuclein (syn211, C20 antibodies) in long-term NAC-treated homozygous DJ-1 mutant neurons at d70. Representative blot shows two biological replicates. GAPDH was used as loading control (n=3). **(D)** T-soluble and T-insoluble α-synuclein (syn303 antibody) in long-term NAC-treated homozygous DJ-1 mutant neurons at d70. Vimentin and GAPDH were used as loading controls. Error bars, mean ± SEM. *$P<0.05$, Student's t-test (A, C).
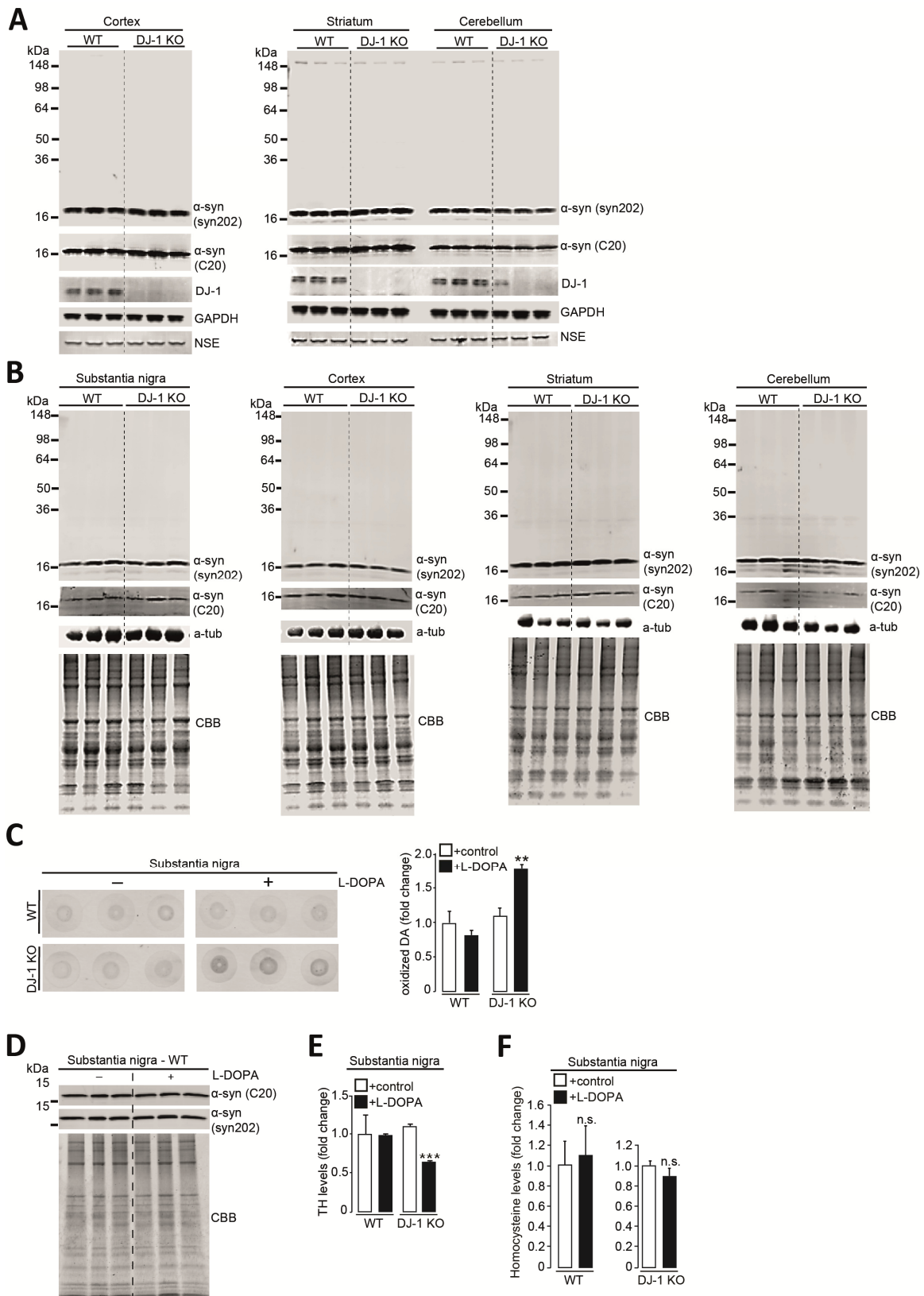
Fig. S7

Fig. S7: Oxidized dopamine and α-synuclein levels in DJ-1 KO and WT mice under basal or L-DOPA treatment conditions. **(A)** Immunoblot analysis of T-soluble α-synuclein extracted from cortex, striatum and cerebellum tissue of DJ-1 KO and WT mice using anti-α-synuclein antibodies syn202 and C20. GAPDH and NSE were used as loading controls (n=3 per group). **(B)** T-insoluble α-synuclein extracted from substantia nigra, cortex, striatum and cerebellum tissue of DJ-1 KO and WT mice using anti-α-synuclein antibodies syn202 and C20. α-tubulin and CBB were used as loading controls (n=3 per group). **(C)** WT and DJ-1 KO mice were fed L-DOPA-supplemented or vehicle-treated chow for 30 days. Their substantia nigra was analyzed at 3-5 months of age for oxidized dopamine (DA) by nIRF. Representative nIRF assay samples are shown (n=6-8 per group). **(D)** WT mice were fed L-DOPA-supplemented or vehicle-treated chow for 6 months. Their substantia nigra was analyzed at 14 months of age. Immunoblot analysis shows T-insoluble α-synuclein levels using anti-α-synuclein antibodies C20 and syn202. CBB was used as loading control (n=3 per group). **(E)** WT and DJ-1 KO mice were fed L-DOPA-supplemented or vehicle-treated chow for 6 months. Their substantia nigra was analyzed at 14 months of age for TH levels by immunoblot (n=3-4 per group). **(F)** Homocysteine levels were measured in supernatants of homogenates derived from nigral tissue of 14 month old WT and DJ-1 KO mice fed with L-DOPA-supplemented or vehicle-treated chow for 6 months (n=3-4 per group). Equal protein concentrations were used for nIRF assays. Error bars, mean ± SEM. **$P<0.01$, ***$P<0.001$, Student's t-test (E-F) or one-way ANOVA with Tukey post-hoc test (C). n.s. = not significant.
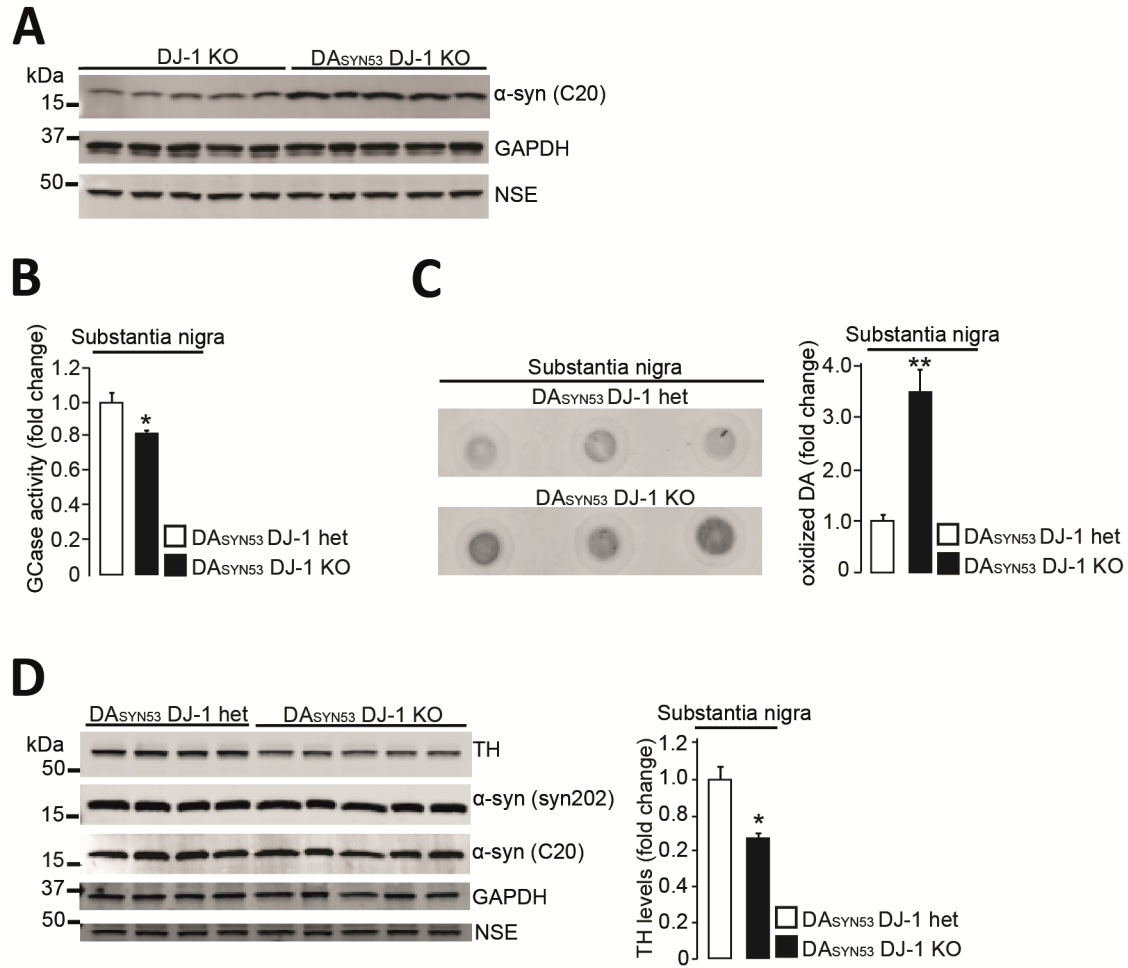
Fig. S8

A

B

C

D

Fig. S8: Analysis of nigral tissue from *DJ-1* KO mice, DA_{SYN53} x *DJ-1* KO mice and DA_{SYN53} x *DJ-1* het mice. **(A)** Immunoblot analysis of α-synuclein levels (C20 antibody) in nigral tissue from *DJ-1* KO and DA_{SYN53} x *DJ-1* KO mice. GAPDH and NSE were used as loading controls (n=5 per group). **(B-D)** Nigral tissue from DA_{SYN53} x *DJ-1* het and DA_{SYN53} x *DJ-1* KO mice was analyzed at 8 months of age for (B) GCase activity, (C) oxidized dopamine by nIRF and (D) TH and α-synuclein (syn202 and C20 antibodies) levels. GAPDH and NSE were used as loading controls. Statistics for TH levels are shown (n=4-5 per group). Equal protein concentrations were used for nIRF assays. Error bars, mean ± SEM. *$P<0.05$, **$P<0.01$, Student's t-test (B-D).

Fig. S9
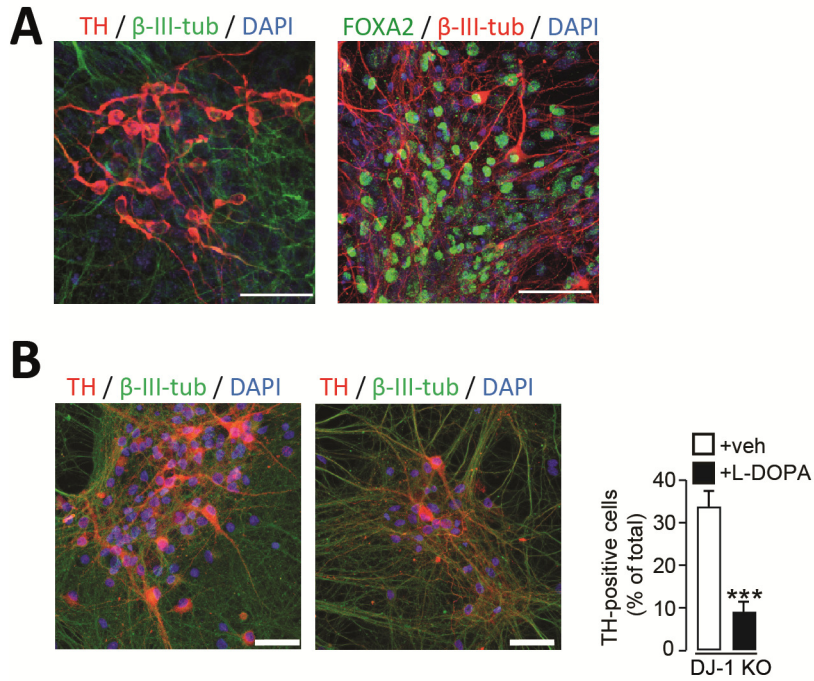
Figure S9: Mouse iPSC-derived neuron characterization. **(A)** Representative immunocytochemical images of dopamine, midbrain and neuronal markers in neurons from iPSC-derived mouse neurons at d40. Antibodies against TH, FOXA2 and β-III-tubulin were used. Scale bar, 50μm. **(B)** *DJ-1* KO mouse iPSC-derived dopaminergic neurons treated with 50 μM L-DOPA or vehicle HCl (from d40-d55) were analyzed at d55 for immunofluorescence of TH (red), β-III-tubulin (green) and nuclear DAPI (blue) (n=3). Scale bar, 50μm. Error bars, mean ± SEM. ***$P<0.001$, Student's t-test (B).
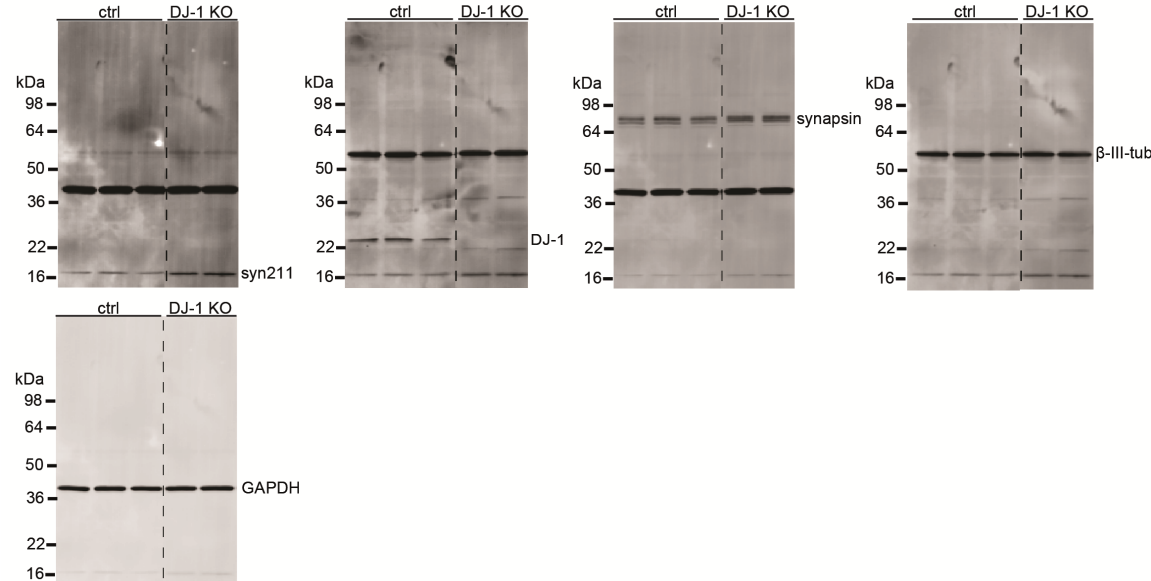
Fig. S10
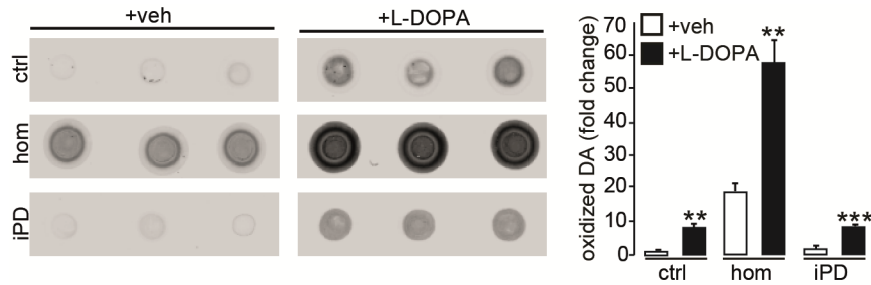
Fig. S10: Accumulation of oxidized dopamine after treatment with L-DOPA in control, homozygous DJ-1 mutant and idiopathic PD neurons. Control, homozygous DJ-1 mutant and idiopathic PD dopaminergic neurons were treated with 50 μM L-DOPA or vehicle (veh) for 20 days and their amount of oxidized dopamine was analyzed by nIRF at d70 (n=3). Quantification for each L-DOPA-treated line is normalized to vehicle-treated condition. Samples included in nIRF assays were loaded based on equal protein concentration. Error bars, mean ± SEM. **$P<0.01$, ***$P<0.001$, Student's t-test.
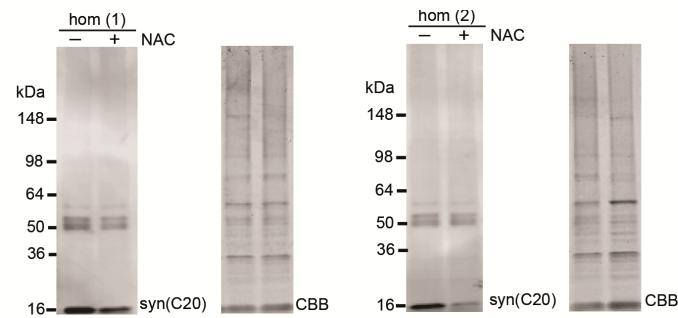
Supplementary Text

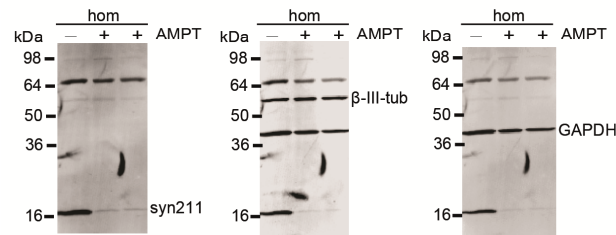## Immunoblots - Figure 3F
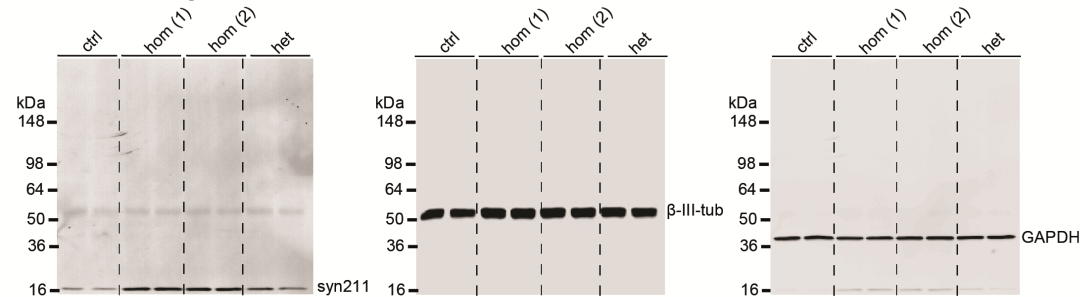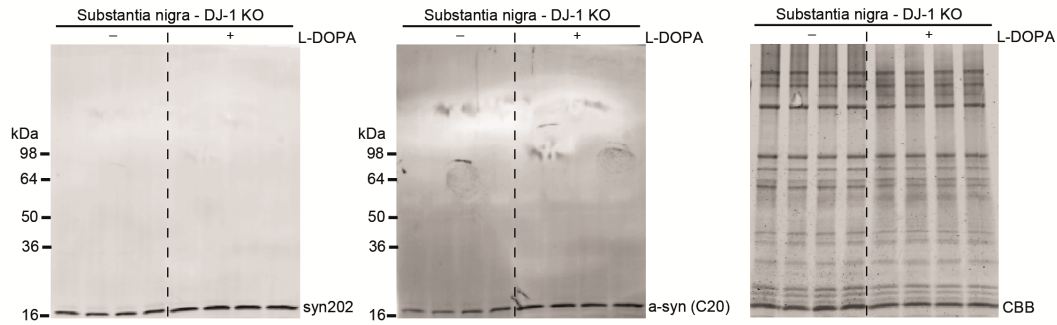

Immunoblots - Figure 3G

Immunoblots - Figure 3H
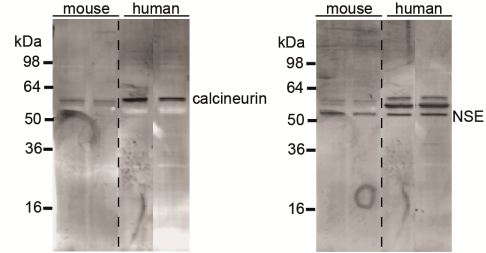

Immunoblots - Figure 3K

Immunoblots - Figure 4C

Substantia nigra
WT   DJ-1 KO

kDa
150 —
100 —
75 —
50 —
37 —
25 —
20 —
15 —   syn(C20)

Substantia nigra
WT   DJ-1 KO

kDa
150 —
100 —
75 —
50 —
37 —
25 —
20 —
15 —   DJ-1

Substantia nigra
WT   DJ-1 KO

kDa
150 —
100 —
75 —
50 —
37 —   GAPDH
25 —
20 —
15 —

Substantia nigra
WT   DJ-1 KO

kDa
150 —
100 —
75 —
50 —   NSE
37 —
25 —
20 —
15 —

Immunoblots - Figure 4H

Substantia nigra - DJ-1 KO
− | +   L-DOPA

kDa
98 —
64 —
50 —
36 —
16 —   syn202

Substantia nigra - DJ-1 KO
− | +   L-DOPA

kDa
98 —
64 —
50 —
36 —
16 —   a-syn (C20)

Substantia nigra - DJ-1 KO
− | +   L-DOPA

CBB

Immunoblots - Figure 5D

mouse   human

kDa
98 —
64 —
50 —   calcineurin
36 —
16 —

mouse   human

kDa
98 —
64 —
50 —   NSE
36 —
16 —

Author Contributions

D.K. was responsible for the overall direction of the experiments, analysis of data and communication of the results. L.F.B. was responsible for the design, strategy and execution of experiments, construction of figures as well as the analysis of results. P.S. was responsible for treatment of mice with L-DOPA and preparation of mouse brains. J.R.M. participated in the design, analysis and communication of the results as well as helped with the HPLC analysis. E.Z. and D.J.S. conducted the electrophysiological experiments. J.B. helped with perfusion and sectioning of mice. S.J. provided technical assistance for differentiation of human iPSCs into dopaminergic neurons. C.D.O. and R.K. were responsible for reprogramming of DJ-1 mutant fibroblasts into iPSCs. D.P.S and E.K designed and performed the CRISPR/Cas9 gene-editing experiments. C.S. and J.N.S. designed and performed the tandem mass spectrometry experiments. X.Z. generated the DA$_{SYN53}$ x DJ-1 KO mice. L.F.B., Y.C.W., D.J.S. and D.K. wrote the paper.

References and Notes

1. L. V. Kalia, A. E. Lang, Parkinson's disease. *Lancet* **386**, 896–912 (2015). doi:10.1016/S0140-6736(14)61393-3 Medline

2. D. J. Surmeier, J. A. Obeso, G. M. Halliday, Selective neuronal vulnerability in Parkinson disease. *Nat. Rev. Neurosci.* **18**, 101–113 (2017). doi:10.1038/nrn.2016.178 Medline

3. T. M. Dawson, H. S. Ko, V. L. Dawson, Genetic animal models of Parkinson's disease. *Neuron* **66**, 646–661 (2010). doi:10.1016/j.neuron.2010.04.034 Medline

4. V. Bonifati, P. Rizzu, M. J. van Baren, O. Schaap, G. J. Breedveld, E. Krieger, M. C. Dekker, F. Squitieri, P. Ibanez, M. Joosse, J. W. van Dongen, N. Vanacore, J. C. van Swieten, A. Brice, G. Meco, C. M. van Duijn, B. A. Oostra, P. Heutink, Mutations in the *DJ-1* gene associated with autosomal recessive early-onset parkinsonism. *Science* **299**, 256–259 (2003). doi:10.1126/science.1077209 Medline

5. J. N. Guzman, J. Sanchez-Padilla, D. Wokosin, J. Kondapalli, E. Ilijic, P. T. Schumacker, D. J. Surmeier, Oxidant stress evoked by pacemaking in dopaminergic neurons is attenuated by DJ-1. *Nature* **468**, 696–700 (2010). doi:10.1038/nature09536 Medline

6. G. Krebiehl, S. Ruckerbauer, L. F. Burbulla, N. Kieper, B. Maurer, J. Waak, H. Wolburg, Z. Gizatullina, F. N. Gellerich, D. Woitalla, O. Riess, P. J. Kahle, T. Proikas-Cezanne, R. Krüger, Reduced basal autophagy and impaired mitochondrial dynamics due to loss of Parkinson's disease-associated protein DJ-1. *PLOS ONE* **5**, e9367 (2010). doi:10.1371/journal.pone.0009367 Medline

7. J. N. Guzman, J. Sánchez-Padilla, C. S. Chan, D. J. Surmeier, Robust pacemaking in substantia nigra dopaminergic neurons. *J. Neurosci.* **29**, 11011–11019 (2009). doi:10.1523/JNEUROSCI.2519-09.2009 Medline

8. L. Zecca, C. Bellei, P. Costi, A. Albertini, E. Monzani, L. Casella, M. Gallorini, L. Bergamaschi, A. Moscatelli, N. J. Turro, M. Eisner, P. R. Crippa, S. Ito, K. Wakamatsu, W. D. Bush, W. C. Ward, J. D. Simon, F. A. Zucca, New melanic pigments in the human brain that accumulate in aging and block environmental toxic metals. *Proc. Natl. Acad. Sci. U.S.A.* **105**, 17567–17572 (2008). doi:10.1073/pnas.0808768105 Medline

9. D. Sulzer, J. Bogulavsky, K. E. Larsen, G. Behr, E. Karatekin, M. H. Kleinman, N. Turro, D. Krantz, R. H. Edwards, L. A. Greene, L. Zecca, Neuromelanin biosynthesis is driven by excess cytosolic catecholamines not accumulated by synaptic vesicles. *Proc. Natl. Acad. Sci. U.S.A.* **97**, 11869–11874 (2000). doi:10.1073/pnas.97.22.11869 Medline

10. J. R. Mazzulli, L. F. Burbulla, D. Krainc, H. Ischiropoulos, Detection of free and protein-bound ortho-quinones by near-infrared fluorescence. *Anal. Chem.* **88**, 2399–2405 (2016). doi:10.1021/acs.analchem.5b04420 Medline

11. J. R. Mazzulli, F. Zunke, T. Tsunemi, N. J. Toker, S. Jeon, L. F. Burbulla, S. Patnaik, E. Sidransky, J. J. Marugan, C. M. Sue, D. Krainc, Activation of β-glucocerebrosidase reduces pathological α-synuclein and restores lysosomal function in Parkinson's patient midbrain neurons. *J. Neurosci.* **36**, 7693–7706 (2016). doi:10.1523/JNEUROSCI.0628-16.2016 Medline

12. J. Choi, M. C. Sullards, J. A. Olzmann, H. D. Rees, S. T. Weintraub, D. E. Bostwick, M. Gearing, A. I. Levey, L.-S. Chin, L. Li, Oxidative damage of DJ-1 is linked to sporadic Parkinson and Alzheimer diseases. *J. Biol. Chem.* **281**, 10816–10824 (2006). [doi:10.1074/jbc.M509079200](doi:10.1074/jbc.M509079200) Medline

13. S. Plum, S. Steinbach, J. Attems, S. Keers, P. Riederer, M. Gerlach, C. May, K. Marcus, Proteomic characterization of neuromelanin granules isolated from human substantia nigra by laser-microdissection. *Sci. Rep.* **6**, 37139 (2016). doi:10.1038/srep37139 Medline

14. J. R. Mazzulli, Y.-H. Xu, Y. Sun, A. L. Knight, P. J. McLean, G. A. Caldwell, E. Sidransky, G. A. Grabowski, D. Krainc, Gaucher disease glucocerebrosidase and α-synuclein form a bidirectional pathogenic loop in synucleinopathies. *Cell* **146**, 37–52 (2011). doi:10.1016/j.cell.2011.06.001 Medline

15. J. D. Miller, Y. M. Ganat, S. Kishinevsky, R. L. Bowman, B. Liu, E. Y. Tu, P. K. Mandal, E. Vera, J. W. Shim, S. Kriks, T. Taldone, N. Fusaki, M. J. Tomishima, D. Krainc, T. A. Milner, D. J. Rossi, L. Studer, Human iPSC-based modeling of late-onset disease via progerin-induced aging. *Cell Stem Cell* **13**, 691–705 (2013). doi:10.1016/j.stem.2013.11.006 Medline

16. O. Cooper, H. Seo, S. Andrabi, C. Guardia-Laguarta, J. Graziotto, M. Sundberg, J. R. McLean, L. Carrillo-Reid, Z. Xie, T. Osborn, G. Hargus, M. Deleidi, T. Lawson, H. Bogetofte, E. Perez-Torres, L. Clark, C. Moskowitz, J. Mazzulli, L. Chen, L. Volpicelli-Daley, N. Romero, H. Jiang, R. J. Uitti, Z. Huang, G. Opala, L. A. Scarffe, V. L. Dawson, C. Klein, J. Feng, O. A. Ross, J. Q. Trojanowski, V. M.-Y. Lee, K. Marder, D. J. Surmeier, Z. K. Wszolek, S. Przedborski, D. Krainc, T. M. Dawson, O. Isacson, Pharmacological rescue of mitochondrial deficits in iPSC-derived neural cells from patients with familial Parkinson's disease. *Sci. Transl. Med.* **4**, 141ra90 (2012). doi:10.1126/scitranslmed.3003985 Medline

17. J. R. Mazzulli, F. Zunke, O. Isacson, L. Studer, D. Krainc, α-Synuclein-induced lysosomal dysfunction occurs through disruptions in protein trafficking in human midbrain synucleinopathy models. *Proc. Natl. Acad. Sci. U.S.A.* **113**, 1931–1936 (2016). doi:10.1073/pnas.1520335113 Medline

18. E. V. Mosharov, K. E. Larsen, E. Kanter, K. A. Phillips, K. Wilson, Y. Schmitz, D. E. Krantz, K. Kobayashi, R. H. Edwards, D. Sulzer, Interplay between cytosolic dopamine, calcium, and α-synuclein causes selective death of substantia nigra neurons. *Neuron* **62**, 218–229 (2009). doi:10.1016/j.neuron.2009.01.033 Medline

19. Parkinson Study Group, Phase II safety, tolerability, and dose selection study of isradipine as a potential disease-modifying intervention in early Parkinson's disease (STEADY-PD). *Mov. Disord.* **28**, 1823–1831 (2013). Medline

20. G. Caraveo, P. K. Auluck, L. Whitesell, C. Y. Chung, V. Baru, E. V. Mosharov, X. Yan, M. Ben-Johny, M. Soste, P. Picotti, H. Kim, K. A. Caldwell, G. A. Caldwell, D. Sulzer, D. T. Yue, S. Lindquist, Calcineurin determines toxic versus beneficial responses to α-synuclein. *Proc. Natl. Acad. Sci. U.S.A.* **111**, E3544–E3552 (2014). doi:10.1073/pnas.1413201111 Medline

21. Y. C. Wong, D. Krainc, α-Synuclein toxicity in neurodegeneration: Mechanism and therapeutic strategies. *Nat. Med.* **23**, 1–13 (2017). doi:10.1038/nm.4269 Medline

22. R. Taipa, C. Pereira, I. Reis, I. Alonso, A. Bastos-Lima, M. Melo-Pires, M. Magalhães, DJ-1 linked parkinsonism (PARK7) is associated with Lewy body pathology. *Brain* **139**, 1680–1687 (2016). doi:10.1093/brain/aww080 Medline

23. L. Chen, Z. Xie, S. Turkson, X. Zhuang, A53T human α-synuclein overexpression in transgenic mice induces pervasive mitochondria macroautophagy defects preceding dopamine neuron degeneration. *J. Neurosci.* **35**, 890–905 (2015). doi:10.1523/JNEUROSCI.0089-14.2015 Medline

24. M. E. Gegg, A. H. Schapira, Mitochondrial dysfunction associated with glucocerebrosidase deficiency. *Neurobiol. Dis.* **90**, 43–50 (2016). doi:10.1016/j.nbd.2015.09.006 Medline

25. K. Takahashi, K. Tanabe, M. Ohnuki, M. Narita, T. Ichisaka, K. Tomoda, S. Yamanaka, Induction of pluripotent stem cells from adult human fibroblasts by defined factors. *Cell* **131**, 861–872 (2007). doi:10.1016/j.cell.2007.11.019 Medline

26. R. Hering, K. M. Strauss, X. Tao, A. Bauer, D. Woitalla, E.-M. Mietz, S. Petrovic, P. Bauer, W. Schaible, T. Müller, L. Schöls, C. Klein, D. Berg, P. T. Meyer, J. B. Schulz, B. Wollnik, L. Tong, R. Krüger, O. Riess, Novel homozygous p.E64D mutation in DJ1 in early onset Parkinson disease (PARK7). *Hum. Mutat.* **24**, 321–329 (2004). doi:10.1002/humu.20089 Medline

27. P. Seibler, J. Graziotto, H. Jeong, F. Simunovic, C. Klein, D. Krainc, Mitochondrial Parkin recruitment is impaired in neurons derived from mutant PINK1 induced pluripotent stem cells. *J. Neurosci.* **31**, 5970–5976 (2011). doi:10.1523/JNEUROSCI.4441-10.2011 Medline

28. S. Kriks, J. W. Shim, J. Piao, Y. M. Ganat, D. R. Wakeman, Z. Xie, L. Carrillo-Reid, G. Auyeung, C. Antonacci, A. Buch, L. Yang, M. F. Beal, D. J. Surmeier, J. H. Kordower, V. Tabar, L. Studer, Dopamine neurons derived from human ES cells efficiently engraft in animal models of Parkinson's disease. *Nature* **480**, 547–551 (2011). Medline

29. S. H. Lee, N. Lumelsky, L. Studer, J. M. Auerbach, R. D. McKay, Efficient generation of midbrain and hindbrain neurons from mouse embryonic stem cells. *Nat. Biotechnol.* **18**, 675–679 (2000). doi:10.1038/76536 Medline

30. L. Chen, B. Cagniard, T. Mathews, S. Jones, H. C. Koh, Y. Ding, P. M. Carvey, Z. Ling, U. J. Kang, X. Zhuang, Age-dependent motor deficits and dopaminergic dysfunction in DJ-1 null mice. *J. Biol. Chem.* **280**, 21418–21426 (2005). doi:10.1074/jbc.M413955200 Medline

31. X. Lin, L. Parisiadou, X.-L. Gu, L. Wang, H. Shim, L. Sun, C. Xie, C.-X. Long, W.-J. Yang, J. Ding, Z. Z. Chen, P. E. Gallant, J.-H. Tao-Cheng, G. Rudow, J. C. Troncoso, Z. Liu, Z. Li, H. Cai, Leucine-rich repeat kinase 2 regulates the progression of neuropathology induced by Parkinson's-disease-related mutant α-synuclein. *Neuron* **64**, 807–827 (2009). doi:10.1016/j.neuron.2009.11.006 Medline

32. D. I. Dryanovski, J. N. Guzman, Z. Xie, D. J. Galteri, L. A. Volpicelli-Daley, V. M.-Y. Lee, R. J. Miller, P. T. Schumacker, D. J. Surmeier, Calcium entry and α-synuclein inclusions elevate dendritic mitochondrial oxidant stress in dopaminergic neurons. *J. Neurosci.* **33**, 10154–10164 (2013). doi:10.1523/JNEUROSCI.5311-12.2013 Medline

33. S. Kaushik, A. M. Cuervo, Methods to monitor chaperone-mediated autophagy. *Methods Enzymol.* **452**, 297–324 (2009). [doi:10.1016/S0076-6879(08)03619-7](doi:10.1016/S0076-6879(08)03619-7) Medline

34. J. E. Elias, S. P. Gygi, Target-decoy search strategy for increased confidence in large-scale protein identifications by mass spectrometry. *Nat. Methods* **4**, 207–214 (2007). doi:10.1038/nmeth1019 Medline

35. J. K. Eng, A. L. McCormack, J. R. Yates, An approach to correlate tandem mass spectral data of peptides with amino acid sequences in a protein database. *J. Am. Soc. Mass Spectrom.* **5**, 976–989 (1994). [doi:10.1016/1044-0305(94)80016-2](doi:10.1016/1044-0305(94)80016-2) Medline

36. J. E. Duda, B. I. Giasson, M. E. Mabon, V. M. Lee, J. Q. Trojanowski, Novel antibodies to synuclein show abundant striatal pathology in Lewy body diseases. *Ann. Neurol.* **52**, 205–210 (2002). [doi:10.1002/ana.10279](doi:10.1002/ana.10279) Medline